journal

J. Am. Ceram. Soc., 83 [8] 1905–13 (2000)

Polyelectrolyte Effects on the Rheological Properties of Concentrated Cement Suspensions

Jennifer A. Lewis,* Hiro Matsuyama, Glen Kirby,* Sherry Morissette,* and J. Francis Young*

Materials Science and Engineering Department, University of Illinois, Urbana, Illinois 61801

Polyelectrolyte species, known as superplasticizers, dramatically affect the rheological properties of dense cement suspensions. We have studied the influence of sulfonated naphthalene formaldehyde condensate (SNF) and carboxylated acrylic ester (CAE) grafted copolymers of varying molecular architecture on the surface (e.g., adsorption behavior and zeta potential) and rheological properties of concentrated cement suspensions of white portland cement and two model compounds, β-Ca_2SiO_4 and γ-Ca_2SiO_4. The adsorption of SNF species was strongly dependent on cement chemistry, whereas CAE species exhibited little sensitivity. The respective critical concentrations (Φ^*) in suspension required to promote the transition from strongly shear thinning to Newtonian flow (flocculated $\rightarrow$ stable) behavior were determined from stress viscometry and yield stress measurements. Theoretical analysis of interparticle interactions suggested that only colloidal particles in the size range of $\leq$1 μm are fully stabilized by adsorbed polyelectrolyte species. Our observations provide guidelines for tailoring the molecular architecture and functionality of superplasticizers for optimal performance.

I. Introduction

POLYELECTROLYTE admixtures, commonly referred to as superplasticizers by the concrete industry, are widely used to improve the flowability of cement-based systems.[1] Sulfonated naphthalene formaldehyde (SNF) and sulfonated melamine formaldehyde (SMF) condensates represent the first generation of superplasticizers and remain in widespread use. Such admixtures, however, suffer a rapid loss of concrete paste flowability over time. This property, known as slump loss, defines the working time associated with placing fresh concrete. A new class of superplasticizers, based on carboxylated acrylic ester (CAE)-grafted copolymers, have been developed that appear to minimize slump loss, thereby significantly extending working time.[2–4] Despite their promising features, the mechanism by which these new additives enhance cement paste flowability remains unclear. This fundamental knowledge is required to provide guidelines for tailoring their molecular architecture (e.g., anchor block molecular weight, fraction ionizable groups, graft chain length, etc.) to further enhance performance.

Polyelectrolyte species can be oligomeric or polymeric in nature, often consisting of both ionizable and neutral side groups attached at frequent intervals along the backbone of a carbon–carbon chain. When adsorbed on inorganic surfaces, these species can impart electrostatic and steric stabilization to the resulting system, known collectively as electrosteric stabilization.[5] In the nonadsorbed state, these species can induce either depletion flocculation or stabilization, depending on their concentration in solution, their charge, and the relative size ratio between the cementitious particles and additives.[6] The relative importance of these individual contributions on the stability of dense cement suspensions has not been established fully because of the complex nature of such systems. Experimental difficulties stem from both the colloidal phase, which undergoes hydration reactions in the presence of water simultaneously altering the surface chemistry and solution composition, and the polyelectrolyte species, whose extent of ionization and adsorption depends strongly on such conditions.

Previous studies conducted on dilute, portland cement suspensions containing SNF species have reported a high, negative value of zeta potential (roughly –30 to –50 mV).[2,7–9] Based on these results, electrostatic stabilization has been proposed as the primary stabilization mechanism for SNF. Preliminary studies[2,3,10] of the new CAE additives have revealed that such species yield significantly lower, negative zeta-potential values, suggesting that the steric contribution may be more relevant. However, a systematic investigation of the influence of such species on the stability of concentrated cement suspensions has not been conducted.

The aim of the present work is to study the effects of superplasticizer additions on the stability of dense suspensions of ordinary white portland cement powder as well as two model compounds, β-Ca_2SiO_4 and γ-Ca_2SiO_4. β-Ca_2SiO_4 is one of the primary cementitious phases present in white portland cement, and γ-Ca_2SiO_4 is its nonhydrating polymorph. Use of model compounds allows system complexity to be reduced to a single colloidal phase of varying reactivity.

Three CAE superplasticizers of varying molecular architecture were characterized along with a traditional SNF admixture, which served as a benchmark in this study. First, experiments were conducted to assess the adsorption behavior and resulting zeta potential of each system. Next, the rheological properties (both stress viscometry and yield stress behavior) of dense cement suspensions of varying superplasticizer concentration were measured. Finally, to aid our interpretation of these results, an analysis of the colloidal interactions in these systems was conducted that accounts for contributions from long-range van der Waals, electrostatic, and steric interactions. We show that steric forces are likely the dominant mechanism by which stability is imparted, but that only fine colloidal particles ($\leq$1 μm) appear to be fully stabilized by the adsorbed species. Our analysis suggests that fine colloidal particles along with nonadsorbed superplasticizer species impart stability to larger particles in suspension via depletion interactions. With this knowledge, design criteria for optimizing the molecular architecture of polyelectrolyte-based superplasticizers is discussed.

II. Experimental Procedure

(1) Materials System

An ASTM Type I white portland cement (Lehigh Portland Cement Co., Allentown, PA) is used in this study. The chemical composition of white cement and the calculated compound composition in this cement determined by XRF analysis are shown in

G. W. Scherer—contributing editor

Manuscript No. 189250. Received July 21, 1999; approved December 22, 1999.
Supported by Asahi Chemical Company and the National Science Foundation under Contract No. DMR 94–53446.
*Member, American Ceramic Society.

Table I. β-dicalcium silicate (β-C_2S) and γ-dicalcium silicate (γ-C_2S) are synthesized by the Pechini process[11] and calcined at 1200° and 1400°C, respectively. The surface area and mean particle size of three cement powders are shown in Table II, as determined by BET (Model ASAP 2400, Micrometrics, Norcross, GA) and particle size analysis (Model CAPA-700, Horiba, Ltd., Tokyo, Japan), respectively. β-C_2S and γ-C_2S have the same chemical composition but exhibit markedly different hydration behavior in the presence of water. β-C_2S undergoes hydration reactions similar to white cement, whereas γ-C_2S is essentially inert.

A sulfonated naphthalene formaldehyde (SNF) condensate (Mighty 100, Kao Chemical Co., Tokyo, Japan) and three types of carboxylated acrylic ester (CAE) copolymers (AA1, Advaflow W11139S-1, and Daracem 210/B, W. R. Grace & Co., Cambridge, MA)[12,13] are investigated in this study. Representative structures of SNF and CAE polyelectrolytes are illustrated schematically in Fig. 1. SNF is a homopolymer (average molecular weight ~5400 g/mol), with a monomer unit consisting of a naphthalene ring structure with one ionizable sulfonic acid group. This is an ideal representation, because the commercial SNF product likely contains some branched chains and closed loops as well as a varying number of sulfonate groups along its backbone. CAE is a comblike copolymer consisting of a poly(acrylic acid) (PAA) backbone that contains one ionizable carboxylic acid group per monomer unit to which poly(ethylene oxide)/poly(propylene oxide) (PEO/PPO) chains are grafted. The average molecular weights of the PAA and PEO/PPO blocks are reported to be in the range of 2000–5000 and 700–2000 g/mol, respectively. A summary of the specific CAE molecular structures, as determined from gel permeation chromatography, infrared spectroscopy, and NMR studies, is provided in Table III. Because of the difficulties associated with characterizing the molecular weight of charged polymers, the reported data reflect approximate values.

Note, both Advaflow (CAE2) and Daracem (CAE3) contained a significant fraction of low molecular weight species (~2300 g/mol), which likely correspond to remnant reactant species. To aid our understanding of CAE interactions with cement, we also separately evaluated the effects of pure PAA (Polysciences, Warrington, PA) and PEO/PPO/PEO (Pluronic F-68, BASF, Mt. Olive, NJ) dispersants. The PAA used had a molecular weight of ~5000 g/mol, while the PEO/PPO/PEO triblock had a total molecular weight of 8400 g/mol with a hydrophobic, PPO segment molecular weight of roughly 2000 g/mol.

(2) Adsorption Behavior

The adsorption of SNF and CAE superplasticizers on white portland cement, β-C_2S, and γ-C_2S was characterized using a Total Organic Carbon (TOC) analyzer (Model DC80, Dohmen), which provided quantitative information of the nonadsorbed fraction of such species in solution. Suspensions with a water to cement ratio (w/c) of 0.35 (47 vol% cement) or 1.0 (24 vol% cement) were prepared by adding an appropriate amount of cement powder to an aqueous stock solution of varying superplasticizer concentration. On mixing for 5 min, the suspensions were centrifuged at 15710*g* for 10 min. The supernatant was immediately decanted and diluted with deionized water for the TOC measurement. Several aliquots of each sample were measured, and an average value was reported based on the calibration curve (correlation coefficient, *R*, was 0.998) produced for each superplasticizer

Table I. Chemical and Phase Composition of Type I White Portland Cement

Component	Composition (mass%)
Chemical composition	
SiO_2	21.9
Al_2O_3	4.18
Fe_2O_3	0.08
CaO	66.6
MgO	1.81
K_2O	0.31
Na_2O	0.16
SO_3	2.87
LOI	1.41
Phase composition	
Ca_3SiO_5	68.2
Ca_2SiO_4	11.4
$Ca_3Al_2O_6$	10.9
$Ca_3Al_2Fe_2O_1$	0.24
Gypsum	6.17

Table II. BET Surface Area and Mean Particle Size of Cement Powders

Cement powders	BET surface area (m^2/g)	Mean particle size (μm)
White cement	1.483	8.58
β-C_2S	1.956	0.95
γ-C_2S	0.896	8.85

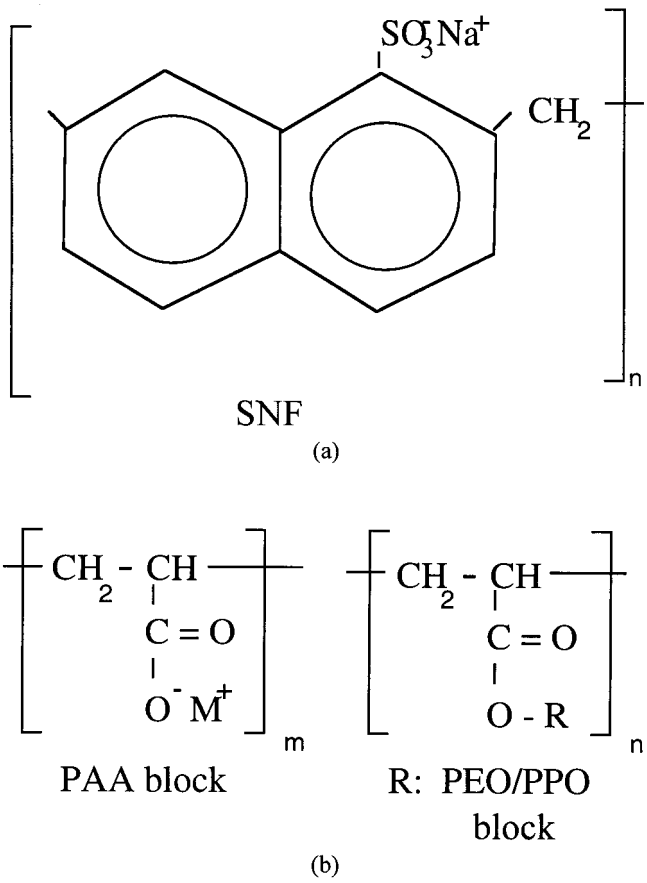

Fig. 1. Schematic illustration of representative molecular structures of (a) SNF and (b) CAE superplasticizers. (Note: $M^+ = Na^+, H^+$; R = $(CH_2CH_2O)_x - (CH_2(CH(CH_3)O)_y - CH_3$, and R group may be alternately grafted via an imidized linkage.)

Table III. Properties of CAE Copolymers

Superplasticizer	MW (g/mol)	Properties		M
		PAA:R	PEO:PPO	
AA1	4 500		1.4:1	Na^+
Advaflow†	15 200	4.8:1	3.5:1	H^+
Daracem†	21 900	2:1	3:1	Na^+

†Significant fractions of low MW chains ~2300 were detected by GPC analysis.

studied. To study the influence of hydration time on adsorption, the mixing time was varied between 5 and 60 min before the centrifugation procedure. The remainder of the procedure was analogous.

(3) Zeta-Potential Analysis

Zeta-potential measurements were performed with a zeta meter equipped with a 30 mL cell (Model ESA-8000, Matec Applied Sciences, Hopkinton, MA). Suspensions with a w/c ratio of 2.0 (13.5 vol% cement) were prepared by adding an appropriate amount of cement powder to an aqueous stock solution of varying polyelectrolyte concentration. Zeta-potential measurements were initiated 5 min after water and cement contact.

(4) Rheological Measurements

Rheological measurements were made using a controlled stress rheometer (Model CS-10, Bohlin Rheologi AB, Lund, Sweden) using the concentric cylinder C-14 bob and cup test geometry (cup diameter 15.4 mm, bob diameter 14.0 mm, bob height 20.0 mm) in either stress viscometry or creep/recovery mode. Concentrated cement suspensions (w/c of 0.25–0.35) were prepared by adding an appropriate amount of cement powder to an aqueous stock solution of varying superplasticizer concentration. The suspensions were hand-mixed for 90 s and then transferred immediately to the sample cup. A specially designed solvent trap was used to minimize the evaporation of water. Each sample was then mixed under high shear at 200 Pa for 45 s. Note, 5 min elapsed between initial water and cement contact (referred to as the hydration time) and this preshearing process. This procedure was adopted to avoid sample handling effects so that each sample had the same shear history.

Stress viscometry measurements were initiated after a hydration time of 11 min following the handling and preshearing steps described above. The applied shear stress was ramped logarithmically down from 150 to 1 Pa and then ramped back up after a 30 s rest from 1 to 150 Pa. A delay time (the time between two consecutive data acquisition events) of 10 s was used in this study. The down/up stress cycle test was completed after roughly 17 min of hydration. The apparent viscosity was also measured at a constant shear stress (50 Pa) as a function of hydration time for representative pastes. In these measurements, data collection commenced 20 s after the completion of the preshearing process, and a delay time of 20 s was used.

A creep/recovery technique is used to measure the yield stress (τ_y) of representative cement pastes as a function of hydration time following the method of Struble and Lei.[14–16] Concentrated cement pastes can exhibit different creep/recovery behavior depending on the applied stress level. At low stress ($\tau < \tau_y$), the pastes behave like an elastic or viscoelastic solid, while at high stress ($\tau \geq \tau_y$), they exhibit an initial elastic response followed by viscous liquidlike behavior. The yield stress of paste is defined by the stress level at which the transition from solid to liquid behavior is observed.

III. Results

(1) Polyelectrolyte Adsorption on White Portland Cement

The adsorption isotherms for SNF and CAE superplasticizers on white portland cement are shown in Fig. 2 for cement suspensions (w/c = 0.35, 47.4 vol% cement) of varying polyelectrolyte concentration. The amount adsorbed onto the cement particle surfaces increased with increasing superplasticizer concentration in suspension until a plateau value (Γ_p) was reached. The values of Γ_p were roughly 4.0, 2.7, 1.5, and 0.7 mg/m^2 for SNF, Advaflow, AA1, and Daracem, respectively. The adsorption isotherms of both Advaflow and Daracem exhibited a shoulder region at $\Gamma \approx 0.5*\Gamma_p$, suggesting that multilayer adsorption could occur for these species. The asterisks shown in Fig. 2 denote the respective critical concentrations (Φ^*) required to promote suspension stability, as determined from rheological behavior. At Φ^*, there was a significant fraction of nonadsorbed species in solution, as revealed by differences between the data shown and the dashed line indicating 100% adsorption. This was quantified for cement suspensions (47.4 vol%) containing the respective critical concentrations (Φ^*) of each superplasticizer species as a function of mixing time in Fig. 3. In as-prepared suspensions (hydration time of 5 min), the percentage of adsorbed superplasticizer ranged from roughly 35%–40% for SNF and Advaflow to 10%–15% for AA1 and Daracem. On mixing for 90 min, the percentage adsorbed increased to 50%–55% for SNF and Advaflow and 20%–30% for AA1 and Daracem. The adsorption of SNF was in reasonable agreement with that reported by Collepardi *et al.*,[2] but our CAE admixtures adsorbed less strongly. Given the similarity in their distribution (adsorbed versus free in solution), the remainder of the experimental work focuses solely on SNF and Advaflow superplasticizers.

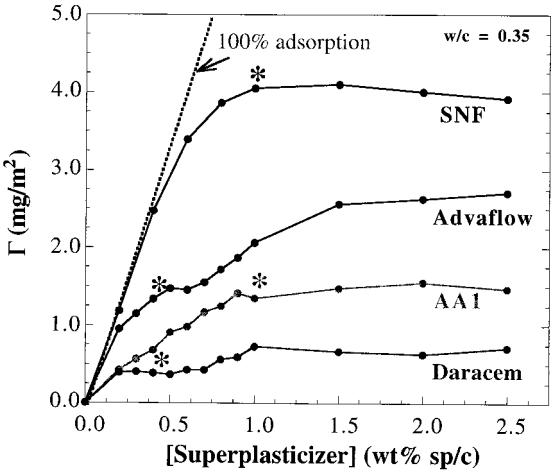

Fig. 2. Initial polyelectroltye adsorption (t = 5 min) on white portland cement as function of superplasticizer concentration in suspension. (Note: Asterisks denote critical concentrations, Φ^*, required to promote suspension stability, as determined from rheological measurements.)

(2) Polyelectrolyte Adsorption on Model Cement Compounds (β-C_2S and γ-C_2S)

The adsorption isotherms for SNF and Advaflow superplasticizers on β-C_2S and γ-C_2S are shown in Figs. 4(a) and (b), respectively, for cement suspensions (w/c = 1.0, 23.9 vol% cement) of varying polyelectrolyte concentration. The adsorption isotherms on white portland cement under analogous conditions

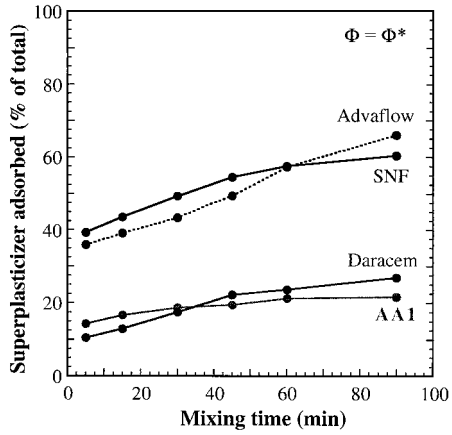

Fig. 3. Relative amount of adsorbed polyelectrolyte on white portland cement as function of hydration time at a superplasticizer concentration in suspension corresponding to respective Φ^* of each system.

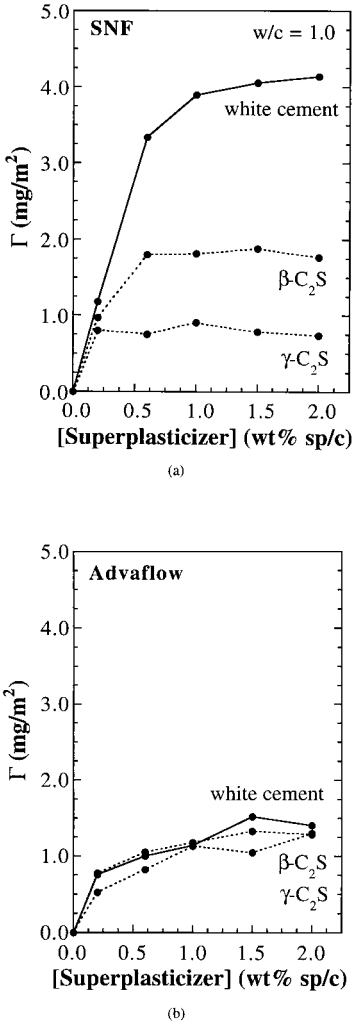

Fig. 4. Initial polyelectroltye adsorption (t = 5 min) on white portland cement, β-C_2S, and γ-C_2S as a function of superplasticizer concentration in suspension: (a) SNF and (b) Advaflow.

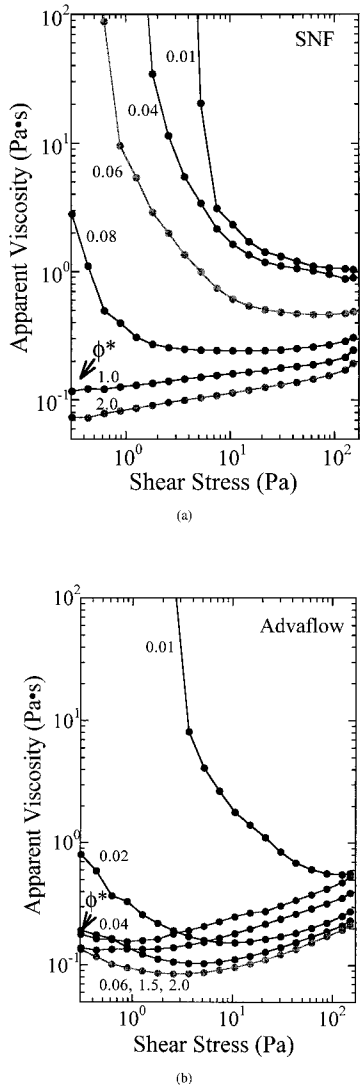

Fig. 5. Log-log plots of apparent viscosity versus shear stress for white portland cement suspensions (w/c = 0.35) of varying superplasticizer concentration (denoted as weight percentage/weight of cement powder): (a) SNF and (b) Advaflow.

are included for comparison. In the case of SNF, the plateau amount adsorbed was strongly dependent on cement reactivity. The values of Γ_p were roughly 4.0, 1.75, and 0.75 mg/m^2 for white portland cement, β-C_2S, and γ-C_2S, respectively. This behavior has been observed previously and was attributed to the presence of tricalcium aluminate (C_3A).[17] In contrast, the adsorption behavior of Advaflow exhibited little sensitivity to cement reactivity, with a Γ_p value of ~1.35 mg/m^2 for all powders investigated.

(3) Polyelectrolyte Effects on Cement Zeta Potential

The zeta potentials (ζ) of white portland cement, β-C_2S, and γ-C_2S suspensions (w/c = 2.0, 13.5 vol% cement) as a function of SNF and Advaflow concentration are reported in Table IV. In the absence of polyelectrolyte admixtures, $\zeta \approx 0 \pm 2$ mV for all samples. At superplasticizer concentrations corresponding to roughly 1.3Φ*, ζ of white portland cement was –7.4 and –2.7 mV for SNF and Advaflow, respectively. Similar values were observed for β-C_2S, where ζ was –5.2 and –0.6 mV for SNF and Advaflow, respectively. In contrast, ζ of γ-C_2S was markedly higher in the case of SNF, where a value of –32.4 mV was observed at 1.3Φ*. Comparing these data to those obtained in earlier studies, two important findings emerged. First, the measured values of ζ of portland cement in the presence of SNF were far lower than the range of values reported previously (i.e., –30 to –50 mV).[7–9] Previous measurements were conducted on very dilute cement suspensions (w/c ≈ 400–1000),[9,18] which gave rise to significant differences in the ionic strength of the solution phase and, hence, differences in the degree of screening between ionized segments. To evaluate this possibility, we conducted measurements using the degree of dilution and SNF concentration reported in Ref. 7 and found a high negative value (ζ = –45.1 mV). Second, the observed differences between the ζ of the cement dispersions in the presence of SNF and Advaflow were only appreciable for the inert cement, γ-C_2S. The origin of these observations is discussed in detail in the following section.

Table IV. Zeta Potential of White Portland Cement, β-C_2S, and γ-C_2S Suspensions

Cements	Additives	Superplasticizer content (wt% s/s) 0	0.2	0.6	1.5
White cement	SNF	1.8	1.5	2.5	−7.4
	Advaflow	1.8	−1.7	−2.7	−2.4
β-C_2S	SNF	−2.1	−9.9	−6.0	−5.2
	Advaflow	−2.1	−0.1	0.6	0.3
γ-C_2S	SNF	−0.6	−40.8	−37.8	−32.4
	Advaflow	−0.6	−6.6	−3.3	−1.5

(4) Polyelectrolyte Effects on Cement Suspension Rheology

Apparent viscosity as a function of shear stress for white portland cement suspensions (w/c = 0.35, 47.4 vol% cement) of

varying SNF and Advaflow concentration is shown in Figs. 5(a) and (b), respectively. For each system, a critical concentration of superplasticizer was identified that corresponded to the amount required to promote the transition from strongly shear thinning behavior ($\Phi < \Phi^*$) to nearly Newtonian flow ($\Phi \geq \Phi^*$) behavior. The values of Φ^* were 1.0 and 0.4 wt% (by weight of cement powder) for SNF and Advaflow, respectively. Modest shear thickening behavior was observed at elevated shear rates for most systems. We attribute such observations to hydrodynamic interactions stemming mainly from nonadsorbed polyelectrolyte chain entanglement.

CAE superplasticizers, such as Advaflow, are comblike copolymers of poly(acrylic acid), PAA, with grafted PEO/PPO chains. To separately evaluate the contribution of each type of segment to cement stability, analogous rheological measurements are conducted for white portland cement suspensions (w/c = 0.35, 47.4 vol% cement) of varying PEO/PPO/PEO and PAA dispersant concentrations. Their respective apparent viscosities as a function of shear stress are shown in Figs. 6(a) and (b). For the concentration range studied, neither PEO/PPO/PEO nor PAA species are able to fully stabilize these suspensions, yielding Newtonian flow behavior. PAA additions yield suspensions with a low shear apparent viscosity several orders of magnitude below that observed for the PEO/PPO/PEO species, suggesting that the former segments are likely to adsorb more strongly onto cement surfaces. From these observations, it is clear that the combination of both PAA segments (which drive adsorption) and grafted PEO/PPO chains (which "stick" out from the cement particle surfaces) is required for effective superplasticizing action.

Yield stress as a function of hydration time for white portland cement suspensions (w/c = 0.35, 47.4 vol% cement) with SNF and Advaflow concentrations both below and above Φ^* is shown in Fig. 7. There is a dramatic rise in yield stress with time for suspensions prepared at ~0.5 Φ^*, with little difference observed between SNF and Advaflow. In contrast, at ~1.3 Φ^*, yield stress increases modestly in the presence of SNF, with no discernible increase in the presence of Advaflow. Such observations likely stem from either differences in dispersion stability and/or hydration kinetics.

IV. Discussion

The experimental results clearly show that polyelectrolyte species strongly influence the rheological behavior, and, hence, stability of concentrated cement suspensions. Firstly, the adsorption behavior of such species on cement particle surfaces is discussed with an emphasis on how molecular structure and hydration phenomena influence this process. Secondly, the stability of such systems in the absence and presence of superplasticizer species is analyzed by accounting for long-range van der Waals, electrostatic, and steric interactions. Finally, the impact of our observations on cement processing as well as strategies for optimizing the design of this important class of polyelectrolyte admixtures are presented.

(1) Polyelectrolyte Adsorption on Cement Surfaces

The adsorption of polyelectrolyte species at the water/cement interface is strongly influenced by the chemical and physical properties of both the solid surfaces and solvent medium.[19] For example, adsorption is strongly favored when polyelectrolytes and the solid surfaces of interest carry opposite charges.[20] At small adsorbed amounts, such species can promote flocculation either by surface charge neutralization or bridging mechanisms. At higher adsorbed amounts, particle stability increases because of long-range repulsive forces stemming from electrosteric interactions.[21] For a given system, the adsorption behavior and conformation of polyelectrolyte species can be modulated by tailoring solvent conditions (e.g., pH and ionic strength). In the case of homopolymers, such as SNF or pure PAA ($pK_a \approx 5$) that have one ionizable group per monomer unit, the degree of ionization (α) increases with increasing pH.[19,20,22,23] Such species adopt a compact coil configuration in solution at low pH ($\alpha \rightarrow 0$) and adsorb in a dense layer of large mass (Γads) and low adlayer thickness (δ), as illustrated in Fig. 8(a). In contrast, under the highly alkaline solution conditions (pH ≈ 12.7) associated with cement systems,

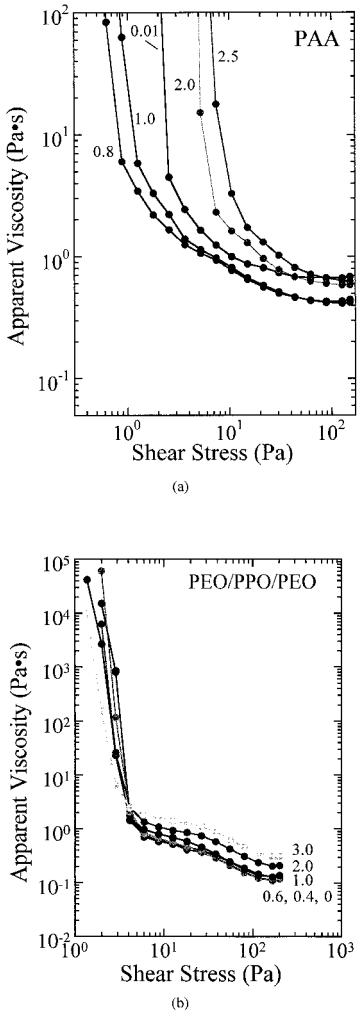

Fig. 6. Log-log plots of apparent viscosity versus shear stress for white portland cement suspensions (w/c = 0.35) of varying model dispersant concentration (denoted as weight percentage/weight of cement powder): (a) PAA and (b) PEO/PPO/PEO.

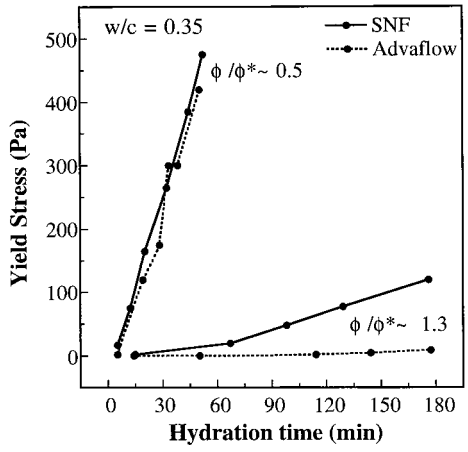

Fig. 7. Yield stress as function of hydration time for white portland cement suspensions (w/c = 0.35) of varying superplasticizer concentration both above and below Φ^*.

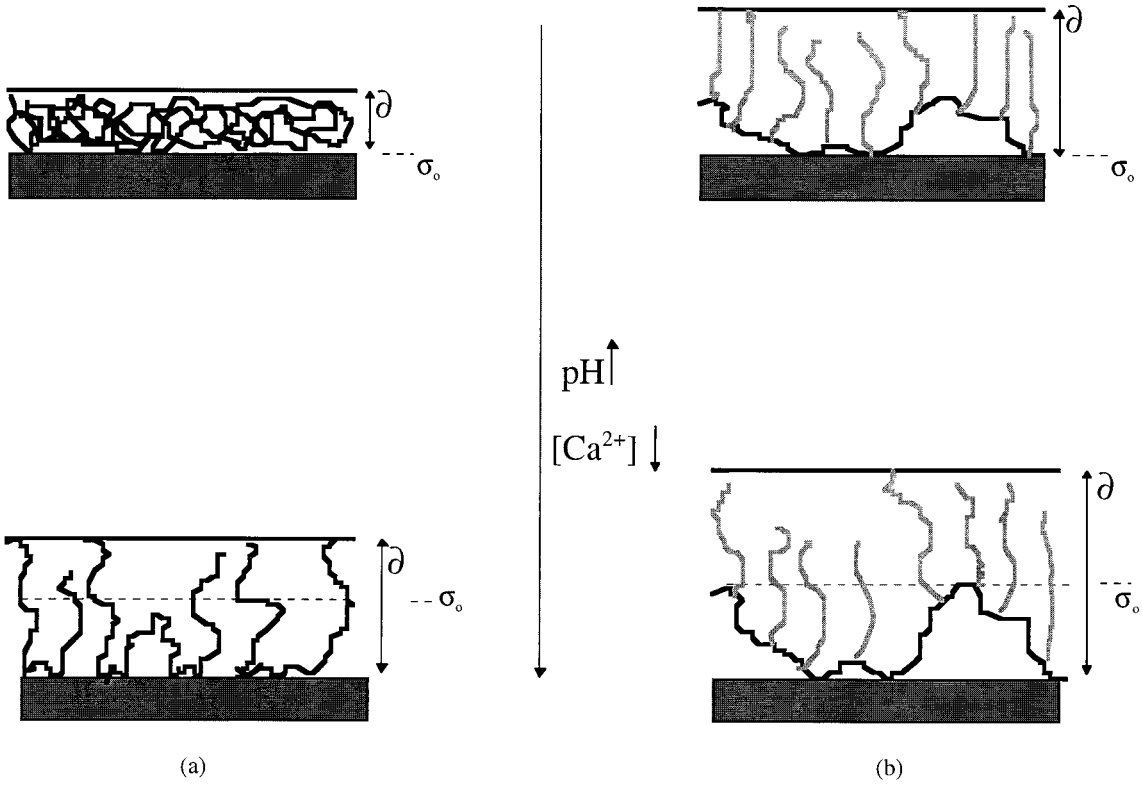

Fig. 8. Schematic illustrations of adsorbed polyelectrolyte species on cement particle surfaces as function of pH and ionic strength: (a) homopolymer, SNF, and (b) copolymer, Advaflow.

one would expect full ionization ($\alpha \rightarrow 1$), resulting in an open coil configuration in solution (because of electrostatic repulsive forces arising between charged segments). Such highly charged species would adsorb in an open layer of low Γads and high δ, also shown in Fig. 8(a).[19,23–25] The actual situation is more complicated, because the aqueous phase of concentrated cement suspensions has a high calcium ion concentration ($[Ca^{2+}] \approx 0.02M$), i.e., it is nearly saturated with respect to $Ca(OH)_2$. Previous work has shown that charge screening effects stemming from divalent ion interactions strongly mitigate intersegment repulsive forces.[22,23,25,27,28] Such interactions are expected to yield a coil configuration and adlayer conformation closer to the low pH regime for superplasticizers, such as SNF.

The experimentally observed adsorption behavior of SNF on white portland cement, β-C_2S, and γ-C_2S is in good agreement with the above view. For example, the plateau adsorbed mass, Γ_{ads}, increases with increasing cement reactivity (i.e., as the ionic strength in solution increases). Direct comparison between the SNF adsorption isotherms on β-C_2S and γ-C_2S best illustrates these trends, because comparison between white portland cement and these model compounds is complicated by the presence of other highly reactive phases (e.g., C_3S and C_3A).[17] The measured ζ of white portland cement, β-C_2S, and γ-C_2S in the presence of SNF lend further support to Ca^{2+}-induced charge screening between polymer segments. A negative ζ of large magnitude is only observed in the case of the inert γ-C_2S compound (or under very dilute conditions, w/c $\approx$ 400–1000 for white portland cement), where the Ca^{2+} ion concentration in solution is negligible.

The sensitivity of both adsorption behavior and adlayer conformation to solution conditions is expected to be lower for CAE polyelectrolytes because of their copolymeric nature. Because only PAA segments along the polyelectrolyte backbone undergo ionization (and these interact strongly with the cement particle surface), the Γads and δ should be less dependent on such conditions. For example, it is expected that the solvation of the PEO/PPO block as well as its molecular weight and graft density are the most critical parameters governing adlayer properties, as shown in Fig. 8(b). The experimentally observed adsorption behavior of Advaflow on white portland cement, β-C_2S, and γ-C_2S is in good agreement with this hypothesis, as there appears to be little effect of cement reactivity on the plateau adlayer mass (Γ_{ads}). The measured ζ values of the cement systems in the presence of Advaflow and SNF also reflect the differences in their molecular architecture, namely in the number of ionizable groups per macromolecule. This point is best illustrated by comparing the measured ζ values for γ-C_2S, where ζ is roughly an order of magnitude lower in the presence of Advaflow compared with SNF at the same relative concentration of $1.3\Phi^*$ or at the same absolute concentration of 1.5 wt%. As expected, such differences diminish with increasing cement reactivity because of the stronger sensitivity of SNF properties to ionic strength.

(2) Theoretical Modeling of Polyelectrolyte–Cement Interactions

Colloidal stability is governed by the total interaction of potential energy, V_{tot}, which may be expressed for the system of interest as the sum of the following contributions:[6]

$$V_{tot} = V_{vdw} + V_{elect} + V_{steric} + V_{dep} \quad (1)$$

where V_{vdw} is the attractive potential energy due to long-range van der Waals interactions between particles, V_{elect} the repulsive potential energy arising from electrostatic interactions between charged particle surfaces, V_{steric} the repulsive potential energy arising from steric interactions between particle surfaces coated with adsorbed polymeric species, and, finally, V_{dep} the potential energy stemming from the presence of nonadsorbed polymeric species in solution that may either enhance or reduce suspension stability. The validity of Eq. (1) has not been fully established; however, it is well known to accurately model systems when fewer contributions exist.[29,30]

The attractive van der Waals interaction potential energy, V_{vdw}, exhibits a power law distance dependence whose strength depends

on the dielectric properties of the interacting colloidal particles and intervening medium. For spherical particles of equal size, V_{vdw} is given by the Hamaker expression:[30]

$$V_{vdw} = -\frac{A}{6}\left(\frac{2}{s^2-4} + \frac{2}{s^2} + \ln\frac{s^2-4}{s^2}\right) \quad (2)$$

where s is

$$s = \frac{2a+h}{a} \quad (3)$$

h is the minimum separation between the particle surfaces, a the particle radius, and A the Hamaker constant. A literature value of 1.68×10^{-21} J was used for the Hamaker constant of cement in water.[31] Use of a nonretarded Hamaker constant is only appropriate when such interactions occur over short separation distances (i.e., $h \leq 5$ nm).[32] However, because of the paucity of spectral data for either multiphase white portland cement or C_2S compounds, retardation effects (that yield a distance-dependent A that decays with h) could not be accounted for in the calculations below.

When two identical particles of radius, a, approach one another under conditions of constant potential, the electrostatic repulsive potential energy can be calculated by (valid for $\kappa a > 10$):[30]

$$V_{elect} = 2\pi\varepsilon_r\varepsilon_o a\Psi_0^2 \ln[1 + \exp(-\kappa h)] \quad (4)$$

where ε_r is the dielectric constant of the solvent, ε_o the permittivity of vacuum, ψ_o the surface potential, $1/\kappa$ the Debye–Hückel screening length, and κ is given by:

$$\kappa = \left(\frac{F^2\Sigma_i N_i z_i^2}{\varepsilon_r\varepsilon_o kT}\right)^{1/2} \quad (5)$$

where N_i and z_i are the number density and valence of the counterions of type i, and F the Faraday's constant. The surface potential is taken to be the measured ζ for a given system.

The steric interaction potential energy, V_{steric}, is calculated using expressions developed by Vincent *et al.*[33] for spherical particles with adsorbed polymer layers. Steric interactions arise when particles approach one another at separation distances less than twice the adlayer thickness (δ). Their close approach can be divided into two domains: the interpenetrational domain ($\delta < h < 2\delta$)[1] and the interpenetrational-plus-compressional domain ($h < \delta$)[2]. The pseudohomopolymer and pseudotails models[33] are used to describe the mixing interactions that occur in the region, $\delta < h < 2\delta$, while the uniform segment model is used to describe the mixing and elastic interactions that occur at smaller separations, $h < \delta$. The pseudohomopolymer model accounts for chain conformations other than tails (i.e., trains and loops) that are expected for adsorbed homopolymers, such as SNF, whereas the pseudotails model is appropriate for grafted polymers, such as Advaflow. For the former model, V_{steric} is given by ($\delta < h < 2\delta$):

$$V_{steric,mix} = \frac{32\pi akT(\bar{\phi}_2^a)^2(0.5-\chi)}{5\nu_1\delta^4}\left(\delta - \frac{h}{2}\right)^6 \quad (6)$$

where $\bar{\phi}_2^a$ is the average volume fraction of segments in the adsorbed layer ($\sim$0.25 for SNF and 0.10 for Advaflow), and υ_1 the molar volume of solvent. At smaller interparticle separations (i.e., $h < \delta$), the polymer segment density is assumed to be uniform, and elastic contributions dominate the interaction potential energy. In this domain, V_{steric} is given by the sum of the mixing ($V_{steric,mix}$) and elastic ($V_{steric,el}$) terms:

$$V_{steric,mix} = \frac{4\pi a\delta^2 kT(\bar{\phi}_2^a)^2(0.5-\chi)}{\nu_1}\left(\frac{h}{2\delta} - \frac{1}{4} - \ln\frac{h}{\delta}\right)$$

$$V_{steric,el} = \frac{2\pi akT\delta^2\rho_2\bar{\phi}_2^a}{M_2^a}\left\{\frac{h}{\delta}\ln\left[\frac{h}{\delta}\left(\frac{3-h/\delta}{2}\right)^2\right] - 6\ln\left(\frac{3-h/\delta}{2}\right) + 3\left(1-\frac{h}{\delta}\right)\right\} \quad (7)$$

where ρ_2 is the density, and M_2^a the molecular weight of the adsorbed species.

To accurately model colloidal interactions in the presence of polyelectrolyte species, assignments of the van der Waals plane, the plane of charge (σ_o), and the steric interaction length (δ) are of critical importance. Theoretical treatments of such interactions have varied significantly, from assuming that double-layer, van der Waals, and steric forces all originate at the polyelectrolyte–solution interface[27] to assuming that double-layer and van der Waals forces originate at the solid–polyelectrolyte interface and steric forces originate at the polyelectrolyte–solution interface.[26] Recently, Biggs and Healey[19] have directly measured such interactions between ZrO_2 surfaces with adsorbed PAA (MW $\approx$ 2000 g/mol) using atomic force microscopy (AFM). At low pH ($\alpha \rightarrow 0$), they observed that the steric interaction length and calculated plane of charge (estimated from the *F/R* versus separation distance curves) were coincident and occurred $\sim$1 nm away from the bare particle surfaces. As pH increased, they observed a dramatic increase in the steric interaction length, with nearly a 10-fold increase ($\delta \approx 10$ nm) at pH 9. Simultaneously, they found a more modest shift for the calculated plane of charge away from the particle surface, which doubled to $\sim$2 nm under the same pH conditions. As their results illustrated, the plane of charge is often located at some intermediate distance between the solid–polyelectrolyte and polyelectrolyte–solution interfaces. One would expect this location to depend strongly on the molecular architecture and solution properties of a given system.

In our calculations, the van der Waals plane originated at the solid–polyelectrolyte surface, and the plane of charge was taken to be coincident with the polyelectrolyte–solution interface for SNF and with an intermediate value of 0.57δ for Advaflow. This latter value reflected the adlayer thickness estimated from $\delta \approx 0.06$ $(MW)^{1/2}$ [6,34] associated with the PAA segments ($\sim$5000 g/mol) of the CAE copolymer. This expression, which neglects ionization effects, yielded adlayer thicknesses of 4.4 and 7.4 nm for SNF and Advaflow, respectively. In comparison, Biggs and Healey[19] measured an adlayer thickness ranging from 1 to 10 nm over the pH conditions studied, whereas one estimates a value of 2.7 nm for adsorbed PAA ($\sim$2000 g/mol). Given the mitigating effects of divalent ions, such as calcium, this approach seems reasonable.

The calculated total interaction potential energy curves of two identical cement particles of varying diameter (D) in the presence and absence of SNF and Advaflow species are shown in Figs. 9 and 10, respectively. For each system, the effects of (a) double-layer and (b) steric forces were separately evaluated. All curves exhibited a shallow secondary minimum of varying magnitude, thus giving rise to differences in colloidal stability. In the case of SNF, calculated well depths of –1.3 kT ($D = 1$ μm) and –13.2 kT ($D = 10$ μm) and of –1.6 kT ($D = 1$ μm) and –19.2 kT ($D = 10$ μm) were observed for double-layer and steric interactions, respectively. In the case of Advaflow, calculated well depths of –1.5 kT ($D = 1$ μm) and –15.4 kT ($D = 10$ μm) and of –0.9 kT ($D = 1$ μm) and –11.3 kT ($D = 10$ μm) were observed for double-layer and steric interactions, respectively. One striking feature of these calculations is that only colloidal particles in the size range of $\leq$1 μm appear to be fully stabilized by adsorbed polyelectrolyte species. The relative importance of double-layer versus steric forces is difficult to discern, because the electrostatic contribution depends strongly on the origin of the plane of charge. Here, we purposely assign this plane to coincide with the polyelectrolyte–solution interface, thereby maximizing the electrostatic contribution for SNF. Given previous experimental work,[19] it is quite likely that this plane is located much closer to the solid–polyelectrolyte surface, thereby relegating electrostatic contributions to a negligible role. In fact, steric interactions alone are sufficient to yield dispersed systems ($D \leq 1$ μm) in the presence of either SNF or Advaflow.

One important implication of our findings is that electrosteric interactions do not appear to effectively stabilize cement particles of median size or greater, even though such systems exhibited a Newtonian flow response (indicative of a dispersed suspension) above the respective critical concentrations of SNF and Advaflow.

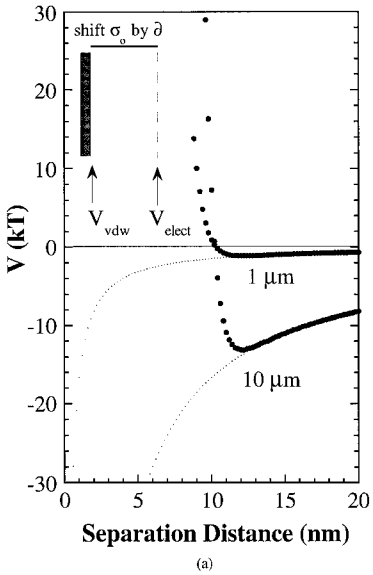

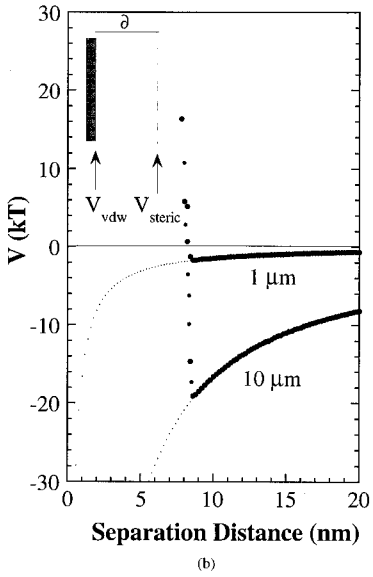

Fig. 9. Calculated potential energy of interaction as function of interparticle separation distance, *h*, for white cement particles of varying diameters with negative zeta potential (–7.4 mV) imparted by adsorbed SNF: (a) DLVO interactions, $V = V_{vdw} + V_{elect}$ (where σ_o is shifted by δ), and (b) steric interactions $V = V_{vdw} + V_{steric}$ (where δ = 4.4 nm). (Note: Small symbols denote long-range attractive V_{vdw} interactions that drive aggregation.)

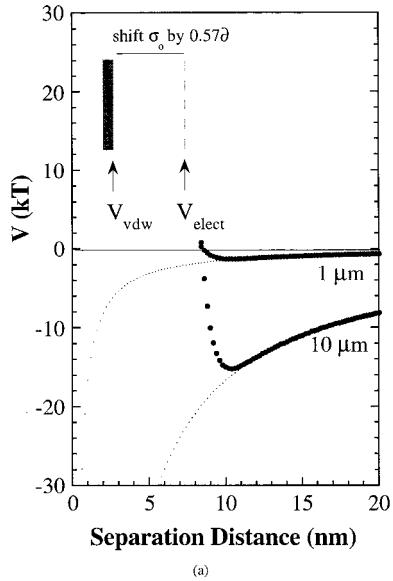

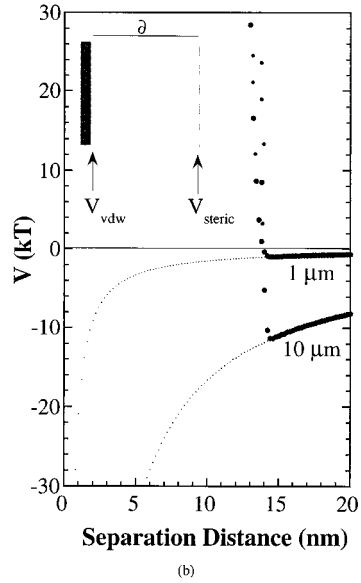

Fig. 10. Calculated potential energy of interaction as a function of interparticle separation distance, *h*, for white cement particles of varying diameters with negative zeta potential (–2.7 mV) imparted by adsorbed Advaflow: (a) DLVO interactions, $V = V_{vdw} + V_{elect}$ (where σ_o is shifted by 0.57δ), and (b) steric interactions $V = V_{vdw} + V_{steric}$ (where δ = 7.4 nm). (Note: Small symbols denote long-range attractive V_{vdw} interactions that drive aggregation.)

This inconsistency between predicted behavior and the measured flow response strongly suggests that additional stabilization mechanisms may be operational, namely depletion forces. It is well known that systems of large particles can be stabilized or flocculated via the addition of nonadsorbed smaller species.[35–38] In the experimental system of interest, both dispersed colloidal particles and polyelectrolyte species present in solution may promote stability. While further work is needed to conclusively demonstrate the role of depletion effects in cement–polyelectrolyte systems, our observations suggest these may be relevant. Hence, when designing the molecular architecture of such molecules for optimal performance, one must consider their role as both adsorbed and nonadsorbed species. In the adsorbed state, the magnitude of the steric interactions at a given length scale depends primarily on steric layer thickness, which increases with polyelectrolyte molecular weight (or grafted chain weight for copolymers), number of ionizable groups per monomer unit, fraction of such groups ionized, etc. In the nonadsorbed state, the magnitude of the depletion interactions depends primarily on the size ratio between the primary (large) colloidal phase and the depletant species as well as their charge. To intensify these interactions, it is desirable to have very low molecular weight, highly charged species.

V. Conclusions

We have shown that polyelectrolyte species, specifically sulfonated naphthalene formaldehyde condensate (SNF) and carboxylated acrylic ester (CAE) grafted copolymers, dramatically affected the rheological properties of dense cement suspensions by promoting a transition from strongly shear thinning to a Newtonian flow response (flocculated → stable) at their respective critical concentrations (Φ^*). Differences in molecular architecture of these macromolecules led to significant differences in their adsorption behavior, zeta potential, and effectiveness as superplasticizer species. The adsorption of SNF, a homopolymer with one ionizable group per monomer unit, depended strongly on cement

chemistry, whereas the adsorption of CAE species exhibited little sensitivity. An analysis of interparticle interactions in these superplasticized cement systems revealed the relative importance of electrostatic, steric, and depletion contributions to colloidal stability. Based on our observations, guidelines have emerged for tailoring the molecular architecture and functionality of such species for optimal performance of concentrated cement dispersions.

Acknowledgments

We kindly acknowledge Mr. Carlos Campos for his assistance with TOC measurements. We thank Asahi Chemical Co. for characterizing the CAE admixtures.

References

[1]V. S. Ramachandran and V. M. Malhotra, 'Superplasticizers"; pp. 211–68 in *Concrete Admixture Handbook*. Noyes, Park Ridge, NJ, 1984.

[2]M. Collepardi, L. Coppola, T. Cerulli, G. Ferrari, C. Pistolesi, P. Zaffaroni, and F. Quek, "Zero Slump Loss Superplasticizer Concrete"; pp. 73–80 in *Proceedings of the Congress of Our World in Concrete and Structures*, Singapore, 1993.

[3]K. Kodama and S. Okazawa, "Development of Superplasticizers for High-Strength Concrete," *Semento Konkuriito*, **546**, 24–32 (1992).

[4]T. Andoh, S. Kase, and S. Tanaka, "Cement Dispersion Effect by Polycarboxylic Acid Type Mixture"; pp. 184–89 in *JCA Proceedings of Cement and Concete.*, Vol. 47. 1993.

[5]R. J. Hunter, *Foundations of Colloid Science*, Vol. 1. Clarendon, Oxford, U.K., 1995.

[6]A. L. Ogden and J. A. Lewis, "Effect of Nonadsorbed Polymer on the Stability of Weakly Flocculated Suspensions," *Langmuir*, **12**, 3413–24 (1996).

[7]P. J. Anderson and D. M. Roy, "The Effect of Adsorption of Superplasticizers on the Surface of Cement," *Cem. Concr. Res.*, **17**, 805–13 (1987).

[8]M. Daimon and D. M. Roy, "Rheological Properties of Cement Mixes: II. Zeta Potential and Preliminary Viscosity Studies," *Cem. Concr. Res.*, **9**, 103–10 (1979).

[9]M. Collepardi, M. Corradi, G. Baldini, and M. Pauri, "Influence of Sulfonate Naphtalene on the Fluidity of Cement Paste"; pp. 20–25 in *VII International Congress On Chemistry and Cements, Paris*, Vol. 3. 1980.

[10]A. Ohta, T. Furusawa, and T. Tsuchitani, "Hydrolysis Mechanism of Crosslinked Polymer Based Superplasticizer with Improved Dispersibility"; pp. 220–25 in *JCA Proceedings of Cement and Concrete*, Vol. 47. 1993.

[11]I. Nettleship, J. L. Shull, and W. K. Kriven, "Chemical Preparation and Phase Stability of Ca_2SiO_4 and Sr_2SiO_4 Powders," *J. Eur. Ceram. Soc.*, **11**, 291–98 (1993).

[12]D. C. Drawin and E. M. Gartner, "Cement Admixture Product," U.S. Pat. No. 5 665 158, 1997.

[13]A. Arfaei and N. H. Milford, "Hydraulic Cement Additives and Hydraulic Cement Compositions Containing Same," U.S. Pat. No. 4 960 465, 1990.

[14]W.-G. Lei, "Rheological Studies and Percolation Modeling of Microstructure Development of Fresh Cement Paste"; Ph.D. Thesis. University of Illinois at Urbana-Champaign, Urbana-Champaign, IL, 1995.

[15]L. J. Struble and W.-G. Lei, "Rheological Changes Associated with Setting of Cement Paste in Advanced Cement Based Materials," *Adv. Cem. Bas. Mater.*, **2**, 224–230 (1995).

[16]W.-G. Lei and L. J. Struble, "Microstructure and Flow Behavior of Fresh Cement Paste," *J. Am. Ceram. Soc.*, **80**, 2021–28 (1997).

[17]V. S. Ramachandran and V. M. Malhotra, pp. 218–20 in *Concrete Admixtures Handbook.* Edited by V. S. Ramachandran. Noyes, Park Ridge, NJ, 1984.

[18]P. J. Anderson, "The Effect of Superplasticizer and Air-Entraining Agent on the Zeta Potential of Cement Particles," *Cem. Concr. Res.*, **16**, 931–40 (1986).

[19]S. Biggs and T. W. Healy, "Electrosteric Stabilization of Colloidal Zirconia with Low Molecular Weight Polyacrylic Acid," *J. Chem. Soc., Faraday Trans.*, **90** [22] 3415–21 (1994).

[20]D. J. Rojas, P. M. Claesson, D. Muller, and R. D. Neuman, "The Effect of Salt Concentration on Adsorption of Low-Charge-Density Polyelectrolytes and Interactions between Polyelectrolyte-Coated Surfaces," *J. Colloid Interface Sci.*, **205**, 77–88 (1998).

[21]J. Marra and M. L. Hair, "Forces between Two Poly(2-Vinyl Pyridine)-Covered Surfaces as a Function of Ionic Strength and Polymer Charge," *J. Phys. Chem.*, **92**, 6044–51 (1988).

[22]L. Jarnstrom and P. Stenius, "Adsorption of Polyacrylate and Carboxy Methyl Cellulose on Kaolinite: Salt Effects and Competitive Adsorption," *Colloids Surf.*, **50**, 47–73 (1990).

[23]V. Hackley, "Colloidal Processing of Si_3N_4 with PAA: I, Adsorption and Electrostatic Interactions," *J. Am. Ceram. Soc.*, **80** [9] 2315–25 (1997).

[24]J. Blaakmeer, M. R. Bohmer, M. A. Cohen Stuart, and G. J. Fleer, "Adsorption of Weak Polyelectrolytes on Highly Charged Surfaces, Poly (acrylic acid) on Polystyrene Latex with Strong Cationic Groups," *Macromolecules*, **23**, 2301–309 (1990).

[25]M. R. Bohmer, O. A. Evers, and J. M. H. M. Scheutjens, "Weak Polyelectrolytes between Two Surfaces: Adsorption and Stabilization," *Macromolecules*, **23**, 2288–301 (1990).

[26]V. Shubin and P. Linse, "Effect of Electrolytes on Adsorption of Cationic Polyacrylamide on Silica: Ellipsometric Study and Theoretical Modeling," *J. Phys. Chem.*, **99**, 1285–91 (1995).

[27]J. M. Berg, P. M. Claesson, and R. D. Neuman, "Interactions between Mica Surfaces in Na-PAA Solutions Containing Ca^{2+} Ions," *J. Colloid Interface Sci.*, **161**, 182–89 (1993).

[28]H. G. M. van de Steeg, M. A. Cohen Stuart, A. D. Keizer, and B. H. Bijsterbosch, "Polyelectrolyte Adsorption: A Subtle Balance of Forces," *Langmuir*, **8**, 2538–46 (1992).

[29]J. E. Seeburgh and J. E. Berg, "Depletion Flocculation of Aqueous Electrosterically-Stabilized Latex Dispersions," *Langmuir*, **10**, 454 (1994).

[30]J. N. Israelachvili, *Intermolecular and Surface Forces*, Academic Press, New York, 1992.

[31]K. Hattori, "Mechanism of Slump Loss and Its Control," *J. Soc. Mater. Sci.*, **29**, [318] 34–40(1970).

[32]J. Mahanty and B. W. Ninham, *Dispersion Forces*. Academic Press, New York, 1976.

[33]B. Vincent, J. Edwards, S. Emmett, and A. Jones, "Depletion Flocculation in Dispersions of Sterically-Stabilised Particles," *Colloids Surf.*, **18**, 261–81 (1986).

[34]D. H. Napper, *Polymeric Stabilization of Colloidal Dispersions*. Academic Press, New York, 1983.

[35]S. Asukara and F. Oosawa, "Interaction between Particles Suspended in Solutions of Macromolecules," *J. Polym. Sci.*, **33**, 183–92 (1958).

[36]J. Clarke and B. Vincent, "Stability of Non-aqueous Microgel Dispersions in the Presence of Free Polymer," *J. Chem. Soc., Faraday Trans.*, **1** [77] 1831 (1981).

[37]J. Y. Walz and A. Sharma, "Effect of Long Range Interactions on the Depletion Force between Colloidal Particles," *J. Colloid Interface Sci.*, **168**, 485 (1994).

[38]Y. Mao, M. E. Cates, and H. N. W. Lekkerkerker, "Depletion Force in Colloidal Systems," *Physica A (Amsterdam)*, **222**, 10 (1995). □